Research Article

Emanuela Muscolino*, Clelia Dispenza

Bio-based hydrogel patches made of κ-carrageenan enriched with degalactosylated xyloglucan for wound dressing applications

https://doi.org/10.1515/bmc-2025-0056 received August 25, 2025; accepted September 1, 2025

Abstract: Hydrogels have become popular for biomedical applications, such as patches and scaffolds for tissue engineering, due to their high-water content, biocompatibility, and tunable physico-chemical and mechanical properties. For instance, chronic wounds remain one of the major global healthcare burdens and, therefore, demand sophisticated ways of managing dressings for fast wound healing to reduce pain, prevent infection, and accelerate healing. κ-Carrageenan (kC) is a polysaccharide extracted from red seaweeds and has been widely considered a promising wound dressing material owing to its biocompatibility and hemostatic properties. Degalactosylated xyloglucan (dXG), obtained through the partial enzymatic removal of galactose from xyloglucan, has demonstrated biocompatibility, anti-inflammatory activity, and excellent scaffolding potential for cells. Both polymers show temperature-induced sol-to-gel transition; however, none of the two form hydrogels that can be used as wound dressings; dXG is too soft, while kC is too brittle, lacking adhesiveness and interconnected porosity. To address these limitations, this study explores interpenetrating hydrogel networks composed of kC and dXG. The resulting kC/dXG hydrogels demonstrate improved mechanical integrity due to the structural contribution of kC, while dXG imparts enhanced swelling capacity and surface adhesiveness. Together, these features make the kC/dXG hydrogel films promising candidates for bioactive wound dressings, yielding hydrogels with good mechanical stability due to kC and enhanced biological properties attributed to dXG.

Clelia Dispenza: Dipartimento di Ingegneria, Università degli Studi di Palermo, Viale delle Scienze, Bldg 6, 90128, Palermo, Italy

Keywords: temperature-responsive polysaccharide, κ-carrageenan; degalactosylated xyloglucan; bioactive wound dressings, wound healing, hydrogel

Introduction

Hydrogels have emerged for various applications in the biomedical field in recent years, for example, as potential candidates for wound dressings, due to their unique features such as high water content, biocompatibility, and tunable characteristics [1-3]. Chronic wounds, such as diabetic foot ulcers, non-healing surgical wounds, or venous leg ulcers, remain a healthcare burden worldwide [4,5]. Efficient dressing of the wound is necessary for quick healing, preventing infections, and reducing pain [6]. κ-Carrageenan (kC) is one of the many hydrogel materials that has been receiving much attention because of its potential in tissue engineering and regeneration medicine. kC is a naturally occurring polysaccharide found mainly in red seaweeds that exhibit good biocompatibility, hemostatic properties, and ability to form films [7–9]. Owing to its backbone conformation, this polysaccharide looks like the innately occurring glycosaminoglycans, which are the central constituents of connective tissues [3,10]. kC is water-soluble at temperatures above 60°C and can set into stable gels with decreasing temperature. The kC networks are stronger in the presence of external metal cations, but networks can also be formed by ionic impurities in the solution [11,12]. Recent studies have shown that kC-based hydrogels, especially when combined with bioactive compounds, can promote more rapid and complete wound closure compared to kC alone [13].

Xyloglucan (XG) is a naturally occurring polysaccharide extracted from tamarind seeds, which is non-ionic, and consists of a backbone of β -(1,4)-D-glucan that is partly modified by α -(1,6)-linked xylose units and might also be partly β -D-galactosylated at the O-2 position. It forms soft, flexible hydrogels at body temperature without the need

^{*} Corresponding author: Emanuela Muscolino, Dipartimento di Ingegneria, Università degli Studi di Palermo, Viale delle Scienze, Bldg 6, 90128, Palermo, Italy; Istituto di Biofisica, Consiglio Nazionale delle Ricerche, Via U. La Malfa 153, 90146, Palermo, Italy, e-mail: emanuela.muscolino@unipa.it

for additives when it is partially degalactosylated (dXG) and mixed with water at fairly low concentrations and temperatures [14–16]. Both XG and dXG might be efficiently customized through radiation to alter their molecular weight distribution, thus adjusting their physicochemical characteristics for various applications [17,18]. Research has already explored dXG as a scaffold that forms *in situ* for cartilage repair [19], as well as an artificial environment for stem cells, demonstrating its capability to maintain cell viability, stemness, and organelle functionality [20–23], or, when combined with specific media, to promote the differentiation of stem cells into osteocytes or chondroblasts [24].

Due to its high adhesive nature, which enables it to act as a glue in plant cell walls, XG finds applications in the biomedical field. It predominantly exhibits adhesive properties through strong hydrogen bonding with cellulose fibers and high water retention capacity, which improve cohesive film or gel formation [25,26]. dXG is formed upon partial elimination of galactose units from XG, increasing the availability of xylose units, thus potentially providing stronger interactions between cellulose and other surfaces [27]. Degalactosylation of XG not only enhances its gelforming ability but also modifies its interaction with immune cells, potentially reducing pro-inflammatory effects, which is advantageous for wound healing applications [28]. dXG also showed increased hydrophobicity, thus adhering very well to hydrophobic surfaces like skin. Both XG and dXG are applied in similar biomedical applications [29]. dXG has been used in several drug delivery systems, where it allows the release of drugs in a sustained way due to its ability to form stable gels. In particular, it has been proposed for the creation of skin patches, for oral [30], ocular [31], and rectal [32] drug delivery devices, and in combination with specific proteins to enhance bioactivity [33,34].

The present study aims at investigating if dXG-enriched kC hydrogel films could be utilized as potential new types of wound dressings. Integration of the innate biocompatibility, film forming capabilities and anti-inflammatory activity of dXG into the kC hydrogels can improve kC porosity, swelling properties, biocompatibility, and the overall efficacy as wound dressings while exploiting the kC structural and mechanical properties to form elastic but still nature-based hydrogels.

This work was designed to study the links between composition, processing, and physicochemical properties of $\kappa C/dXG$ hydrogels as a foundation for biomedical applications with a focus on wound healing. While *in vitro/in vivo* testing lies outside the scope of the present work, the individual polymers used (kC and XG/dXG) are broadly reported as a biocompatible and wound-healing support.

Both polysaccharides have been proven to have excellent biocompatibility in previous studies [20,21,24,35,36] and have been considered for applications in wound dressings [3,37,38]. More specifically, while previous studies have explored the individual applications of kC as a wound dressing [7–9] and the combination of kC with synthetic materials like polyvinyl alcohol [1,39] and polyethylene glycol [2], or with biopolymers such as hyaluronic acid – that has been shown to improve its mechanical properties and efficacy in wound healing applications – Nonetheless, the incorporation of dXG into kC hydrogels for wound dressings remains novel.

Experimental

Materials

kC was provided by Gelcarin ME 8625 FMC Biopolymer. XG from tamarind seeds (sugar composition: glucose, 45% w; xylose, 34% w; galactose, 17% w; arabinose and other sugars, 4% w) was purchased from Megazyme International (Ireland). β -Galactosidase from Aspergillus oryzae (11.8 U/mg) was acquired from Sigma Chemicals (USA). XG from tamarind seeds was degalactosylated (dXG) using a conventional protocol, to gain a degalactosylation degree of ca. 45% [14,40].

Potassium chloride (KCl), sodium azide (NaN₃), potassium bromide (KBr), sodium phosphate dibasic (SFD), sodium chloride (NaCl), and potassium phosphate monobasic (PFM) were purchased from Sigma-Aldrich. A phosphate-buffered saline (PBS) solution was prepared with 0.111% w SFD, 0.85% w NaCl, and 0.032% w PFM. Fetal bovine serum (FBS) was purchased from Mediatech, Inc. lot 35079001. For hydrogel preparation, distilled water was used.

Preparation of polymeric dispersions, solutions, and hydrogels

The compositions of each constituent in the final concentrations of the formulations, along with their corresponding codes, are detailed in Table 1. All formulations contained 0.02% w NaN_3 as a preservative to inhibit mold growth during experimental testing, with the exception of those prepared as references to elucidate the impact of Na^+ on the rheological behavior of kC.

The kC solution (2% w), with and without KCl (0.4% w), was made by maintaining uninterrupted stirring at 80°C for the duration required to attain a clear, homogeneous

Table 1: kC and kC/dXG hydrogel blend codes and compositions

System code	kC (% w)	dXG (% w)	KCI (% w)	NaN ₃ (% w)
kC2	2	_	_	_
kC2-Na	2	_	_	0.02
kC2-K	2	_	0.4	_
kC2-Na-K	2	_	0.4	0.02
kC2/dXGx-Na-K	2	x = 0.25, 0.5, 0.75, 1	0.4	0.02

solution. The polymer blend systems were prepared using three distinct methodologies as outlined below:

First method and second method

dXG solutions at concentrations of 0.5% w, 1% w, 1.5% w, and 2% w were made by adding dXG powder to water prefiltered with 0.22 µm cut-off and stirred for approximately 2 h at 5°C until a homogeneous dispersion was achieved. A kC solution (4% w), also containing KCl (0.8% w), was prepared by maintaining uninterrupted stirring at 80°C for the duration required to obtain a clear, homogeneous solution. Subsequently, the two aqueous polymer solutions were combined in equal volumes and stirred at approximately 120°C in an oil bath on the stove. The pressure inside was maintained by using pressure-resistant bottles with autoclave-suitable caps, and no boiling was visible in the solution even at 120°C. The stirring time was 5 h for the first method or 1h for the second method (used only for the blend containing dXG 2% w). Stirring was ceased once the mixture appeared homogeneous, and the blend was gradually cooled down to room temperature by immersing it in an oil bath tuning off the heating.

Third method

A dXG solution at 2% w was made according to the first method and afterward was stored at 4°C for 48 h. A kC solution (4% w), also containing KCl (0.8% w), was prepared in accordance with the first method procedure. The two aqueous polymers were then mixed in equal volumes and stirred at approximately 120°C for 3 additional hours. The stirring was performed in an oil bath on the stove. The pressure inside was maintained by using pressure-resistant bottles with autoclave-suitable caps, and no boiling was visible in the solution even at 120°C. Mixing was ceased once homogeneity was reached, and the blend was rapidly cooled down to 15°C by putting it in an ice bath.

All solutions prepared with the three methods were stored at room temperature and used over the course of a few weeks.

UV-vis absorbance analysis

The UV-vis absorbance analysis was conducted using an Agilent Technologies Cary 60 UV-vis spectrometer. To prepare the samples for analysis, the kC/dXG hydrogel solutions were heated to 80°C to facilitate the gel-sol transition. Following this, the solutions were transferred into cuvettes and allowed to return to a gel state. The cuvettes were subsequently placed in the UV spectrometer for measurement at room temperature. The cuvette used was quartz with an optical length path of 1 cm.

Fourier transform infrared (FTIR) spectroscopy

FTIR analysis was conducted utilizing a Spectrum Two FTIR spectrometer from Perkin Elmer to examine kC/dXG blends. Each powder system was combined with KBr at a ratio of 1:25. The mixture was subsequently pressed into tablets. The hydrogels were initially freeze-dried, then processed into powders, and combined with KBr in the same ratio of 1:25. These were also shaped into tablets with a hydraulic press before being analyzed on the FTIR spectrometer.

Rheological analysis

Temperature ramps

Temperature ramp measurements were conducted using a stress-controlled rheometer AR G2 (TA Instruments). An acrylic plate with a diameter of 40 mm and a gap of approximately 1,000 µm was utilized for the tests. A quantity of 5 g of each system was heated to 80°C for 15 min, or to 120°C for 15 min, only for the solution made using the third method. The hydrogel solution was then carefully transferred onto the bottom plate of the rheometer. To minimize water evaporation, the sample was surrounded by oil and covered with an appropriate lid. The rheometer temperature was changed from 80 to 30°C and turned back to 80°C at a speed of 1°C/min for all kC2 solutions; for the

kC2/dXGx-Na-K solutions, the temperature was varied from 80 to 30°C at a speed of 1°C/min; and for the kC2/dXG1-Na-K solutions prepared using the third method, the temperature was varied from 90 to 30°C at both 1 and 0.2°C/min. The frequency was maintained at 1 Hz, with the strain set at 8×10^{-4} .

Amplitude sweep and frequency sweep

The amplitude sweep and frequency sweep analyses were conducted using a stress-controlled rheometer AR G2 (TA Instruments). For the small-oscillatory rheological evaluation of kC/dXG systems, 7.5 g of each sample was heated approximately to 80°C for 15 min, or to 120°C for 15 min only for the hydrogel processed via the third method. The resultant blend was then transferred into a Teflon mold and allowed to cool down to room temperature for 10 min. The resultant disk was flipped and positioned on the rheometer plate. Measurements began after 10 min of equilibration time. The geometry employed consisted of an aluminum plate with a diameter of 60 mm and a gap of approximately 2,000 µm. The rheometer temperature was maintained at 37°C. For the amplitude sweep tests, the frequency used was 1 Hz, the strain was varied from 1 × 10⁻⁵ to 0.1, and the strain to maintain a linear viscoelastic behavior was identified as 8×10^{-4} . Subsequently, for the frequency sweep tests, the strain used was 8×10^{-4} , and the frequency was varied from 0.5 to 50 Hz.

Scanning electron microscopy (SEM)

The microstructure of the hydrogels was examined using a field emission scanning electron microscope, Phenom ProX desktop, operated at an accelerating voltage of 10 kV. Prior to analysis, the hydrogels were subjected to freezing in liquid nitrogen, followed by freeze-drying. They were then attached on aluminum stubs and coated with gold using a JFC-1300 gold coater (JEOL) for a duration of 120 s at a current of 30 mA.

Swelling/erosion analyses

In the swelling tests conducted for kC/dXG hydrogels, six samples of each system (approximately 1 g) were weighed using a precision balance. These samples were then covered with 10 mL of either water (containing 0.02% w NaN₃

as a preservative), or PBS, or 3 mL of FBS. Throughout the experiments, the water and FBS solutions remained unchanged, whereas the PBS was refreshed. At predetermined time intervals, samples were carefully extracted from the solution, gently blotted to remove excess liquid, and weighed. The mass change (% MC) was calculated as follows:

$$MC = \frac{W_t - W_i}{W_i} \times 100,$$

where W_t is the hydrogel weight at time t and W_i is the weight at the initial time point.

Adhesive strength analysis

Adhesive strength analysis was performed using a rheometer HR20 Discovery, TA Instruments. The geometry selected was an aluminum plate of 25 mm diameter covered with silicon synthetic skin, with a gap of ~4,000 μm . The test was performed on four samples for each system. They were prepared by cutting hydrogel disks ca. 22 mm diameter and 4 mm height. The samples were pre-compressed to 0.5 N, and then tension was performed with a 30 $\mu m/s$ crosshead rate at 37°C.

Results and discussion

The following results highlight how the properties of the hydrogels, the subject of this study, are influenced by different factors related to composition and preparation. First, the effect of monovalent cations on kC is examined, revealing how ionic type alters its gelation behavior and structural characteristics. The study then explores how different preparation methods affect the interaction between kC and dXG, emphasizing the role of processing conditions in defining the final properties of the blends. Lastly, the impact of varying dXG concentrations within kC systems is assessed, offering insights into how compositional changes influence the gel strength and network formation.

All formulations prepared were subjected to visual inspection to evaluate the color, homogeneity, sheerness, and the incidence of syneresis water. Additionally, qualitative assessments of their handling properties were conducted. Table 2 summarizes the features of each formulation based on visual and tactile inspection. The hydrogels containing dXG exhibited a progressive increase in turbidity with higher concentrations of dXG. In contrast,

the hydrogels that did not contain dXG were observed to be the clearest upon visual inspection.

Influence of K⁺ and Na⁺ ions on kC gelation and properties

kC gelation is enhanced by monovalent cations that grant double helix association by screening the negative charges on the kC chains. For this purpose, the influence of K⁺ and Na⁺ cations on the kC formulations was studied.

First, the functional groups of kC powder and gels were investigated through FTIR analysis. The FTIR signature of kC is described by Volery et al. [41] and presented in Table S1. The results of FTIR measurements conducted on the kC2-Na, kC2-Na-K, and kC powder samples are illustrated in Figure S1. Notably, the FTIR spectrum of the kC powder sample exhibits all the characteristic peaks associated with typical kC, while no indicative peaks of other carrageenans are observed. The characteristic peaks [41] at 1,220 cm⁻¹ for the ester sulfate group, at 928 cm⁻¹ for the 3.6-anhydrogalactose, and at 844 cm⁻¹ for the galactose-4sulfate are present. Upon comparison with the pure kC powder, the kC2-Na and kC2-Na-K hydrogels exhibited similar peaks, although with reduced sharpness and intensity. This observation may be attributed to the involvement of the groups responsible for these peaks in secondary interactions resulting from gelation. A notable distinction between the FTIR spectra of the gels and the powder is the presence of a peak at 2,044 cm⁻¹, which is associated with NaN₃, included in the formulation as a preservative. In addition, the peak corresponding to KCl is likely obscured by the characteristic peaks of kC.

The hydrolytic stability of the systems was evaluated by studying the percentage of mass change of the kC systems kC2-Na and kC2-Na-K. The mass change can be attributed to the combined effects of swelling and erosion, and it

was investigated in both water and PBS, as illustrated in Figure 1a. The results indicated that the kC2-Na formulation initially swelled in water that contained 0.02% w NaN₃ as a preservative; however, it subsequently began to dissolve, with no trace of the gel remaining after 18 h. Numerous studies have demonstrated that kC forms gels in the presence of even trace concentrations of monovalent cations, and the structure of these kC gels is significantly influenced by the type and concentration of such cations [12]. It is well known that Na⁺ leads to a more "disordered" and weaker network with respect to K⁺ [12]. Furthermore, it is present in the swelling medium at a fairly low concentration. As a result, the hydrogel is eventually fully dissolved in water. The same assessment was conducted on the kC2-Na-K system hydrogel. Following a period of swelling, despite the physical crosslinking effect of K⁺ ions, the gel ultimately succumbed to dissolution as well. This outcome suggests that the K⁺ ions, intended to fortify the network, become diluted in distilled water and subsequently leach from the network, resulting in gel dissolution.

To ascertain whether the presence of ions in the swelling medium influenced the degradation of kC2-Na and kC2-Na-K hydrogels, an additional evaluation was conducted using a swelling solution composed of isotonic PBS containing 0.02% w NaN₃ as a preservative. The PBS solution was characterized by a higher concentration of K⁺ ions, although in lesser quantities, compared to those present in the formulations. The results of this test (Figure 1b) revealed a markedly different profile: while the hydrogels demonstrated minimal swelling in the presence of PBS, as opposed to the swelling medium containing solely NaN₃, both samples exhibited a net mass loss of only 10% of the initial weight. This behavior can be justified by the fact that once the hydrogel absorbs sufficient water to facilitate the rearrangement of polymer chains into a double helix structure - incorporating K⁺ ions from the swelling medium the network becomes increasingly ordered and compact, resulting in reduced water uptake [42]. Consequently, the

Table 2: Main hydrogel characteristics from visual analysis

System	Uniformity	Color	Transparency	Optical density at 500 nm	Syneresis	Handling properties
kC2	✓	Slight yellow	+++++	0.18	+++	Hard-brittle
kC2-Na	✓	Slight yellow	+++++	0.18	+++	Hard-brittle
kC2-Na-K	✓	Slight yellow	+++++	0.18	+++	Hard-brittle
kC2/dXG0.25-Na-K	✓	Yellow/white	+++++	0.70	++	Hard-flexible
kC2/dXG0.5-Na-K	✓	Yellow/white	++++	1.30	++	Hard-flexible
kC2/dXG0.75-Na-K	✓	Yellow/white	+++	1.50	++	Hard-flexible
kC2/dXG1-Na-K	✓	Yellow/white	++	1.70	++	Hard-flexible

All parameters are obtained at the temperature of 25°C.

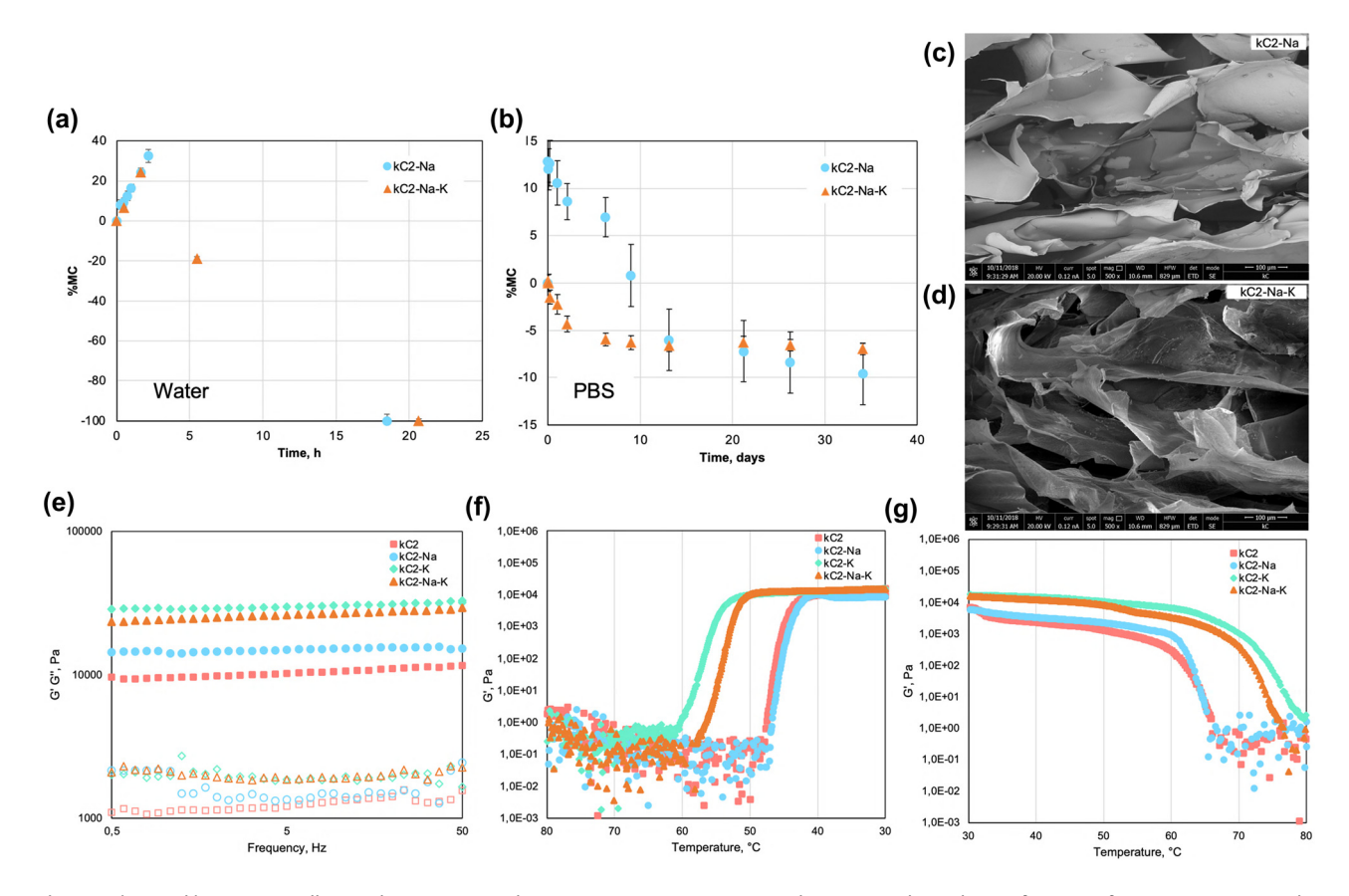


Figure 1: kC2 and kC2-Na-K swelling and erosion mass change, %MC, in 0.02% w NaN₃ solution (a) and PBS (b) as a function of time. SEM micrographs (cross-sections) of kC2-Na (c) and kC2-Na-K (d) at $500\times$ magnification (scale bar: 100μ m). Rheological analysis of kC2, kC2-K, kC2-Na, and kC2-Na-K: (e) storage modulus, G' (full dot), and loss modulus, G'' (hollow dot), as a function of frequency; (f) storage modulus (G') from temperature-sweep, decreasing the temperature at a rate of 1°C/min from 80 to 30°C; (g) storage modulus (G') from temperature-sweep, increasing the temperature from 30 to 80°C.

kC2-Na-K hydrogel, which already contains K^{+} , does not experience the initial swelling.

The mechanical properties of the hydrogels were assessed through dynamic-mechanical frequency sweeps. The analysis involved various kC hydrogel formulations, as illustrated in Figure 1e. Other than kC2-Na and kC2-Na-K hydrogels, this evaluation included kC2 without any cations and kC2-K containing K⁺ ions, to thoroughly assess the effects of these cations on mechanical properties. During these tests, the temperature was maintained at a constant physiological condition of 37°C, while the frequency was varied from 0.5 to 50 Hz.

In all systems analyzed, G' consistently exceeds G'' and remains invariant across frequencies, which is characteristic of relatively strong gels. The kC hydrogel exhibiting the greatest strength is the formulation containing only 0.4% w KCl, despite the G' and G'' moduli being quite similar to those of the formulation incorporating both salts, 0.4% KCl and 0.02% NaN $_3$. This observation can be explained by the fact that K^+ concentration is 20 times

greater than that of Na⁺, coupled with kC higher affinity for K⁺ in comparison to Na⁺. However, the presence of Na⁺ could still sometimes substitute K⁺, introducing a slightly more disordered gel structure, resulting in a marginal decrease in strength, however negligible. It is worth noting that Mangione et al. [12] reported an increase of the viscoelastic moduli upon addition of Na⁺ in the presence of K⁺, whereas in our case the effect of Na⁺ is negligible or slightly destabilizing. This apparent discrepancy can be ascribed to the different experimental regimes: they employed a lower kC concentration (0.4% w) combined with much higher Na⁺ levels (100 mM), conditions under which Na⁺ provides strong electrostatic screening and facilitates aggregation. In contrast, in our system (2% w kC, ~3 mM Na⁺), the network is already strongly stabilized by K+ and the small amount of Na+ is insufficient to provide significant screening but can nonetheless compete with K⁺ causing minor disorder.

The kC hydrogel prepared without any added salts demonstrates the lowest G' and G'' moduli, while the

formulation with a modest concentration of NaN3 exhibits greater strength. Although Na⁺ ions do not induce the same ordered structure with double helix configurations as K⁺ ions, they nonetheless facilitate a degree of organization within the polymer chains, leading to a stronger gel compared to that formed without any salts.

Figure 1f and g depicts the variations in storage modulus for kC2, kC2-K, kC2-Na, and kC2-Na-K hydrogels as a function of temperature, measured at a fixed frequency of 1 Hz with a temperature rate of 1°C per minute. These experiments aimed to analyze the sol-gel transition during cooling from 80 to 30°C (Figure 1f) and the reverse gel-sol transition during heating from 30 to 80°C (Figure 1g). In all cases, the sol-to-gel transition temperature ($T_{\rm sol-gel}$) is notably lower than the gel-to-sol transition temperature $(T_{\text{gel-sol}})$, consistent with findings on pure kC hydrogels [43]. This discrepancy arises due to the higher energy required to break the structural elements responsible for gel formation.

The transition temperatures $T_{\text{sol-gel}}$ and $T_{\text{gel-sol}}$ for kC2 and kC2-Na are nearly identical, suggesting that the presence of NaN₃ has little impact on the sol-gel and gel-sol transitions of the hydrogel. Conversely, in the case of kC2-K, both transition temperatures are significantly higher compared to the gel without KCl, which is consistent with findings reported in the literature [44]. The kC2-Na-K hydrogel exhibited $T_{\text{sol-gel}}$ and $T_{\text{gel-sol}}$ transition temperatures slightly lower than those of kC2-K. This minor difference is primarily due to the significantly higher concentration of KCl - 20 times that of NaN₃. Despite its lower quantity, Na⁺ ions compete with K⁺, leading to a slightly weaker gel compared to kC2-K.

The gel-sol transition temperatures were determined as the point where the G' value deviates by more than 5% from the average of previous measurements, as detailed in Table 3.

Figure 2c and d shows the images of kC2 and kC2-Na-K from the morphological analysis of the structure of our samples, analyzed using a scanning electron microscope. It can be seen that the structure is compact and formed by layers of polymer, it is not influenced by salts, and microporosity is absent.

Table 3: Sol-gel transition temperatures of various systems

System	T (°C)
kC2	44
kC2-Na	43
kC2-K	54
kC2-Na-K	52

Influence of hydrogel preparation method on kC/dXG blends

As already mentioned, kC has a gelation mechanism based on the presence of certain cations, such as K⁺, resulting in the formation of double helices with its polymer chains, and it gels under specific temperature conditions. In contrast, XG can only achieve gelation when it is degalactosylated (dXG) by more than 35% and does so within a defined temperature range of 25-100°C. Given the distinct gelation mechanisms and temperature requirements of kC and dXG, their combination at higher concentrations is not straightforward. To investigate their efficacy and influence on the resulting hydrogel, three different preparation methods - first, second, and third - were employed to formulate kC2/dXG1-Na-K, the formulation with the highest dXG concentration and so the most challenging blending condition.

The FTIR spectra are provided in Figure S2, offering insights into the interactions between the kC and dXG components. The FTIR spectra of the kC and dXG powder mixture in a 2:1 ratio, as well as the individual components (Figure S2a), show that the spectrum of the mixture primarily aligns with that of kC, the major component. The characteristic peaks for XG, documented in Table S2, are also visible. A detailed comparison of kC2-Na-K, kC2/dXG0.5-Na-K, and kC2/dXG1-Na-K (Figure S2b) highlights a reduction in the intensity of peaks associated with kC ester sulfate (1,220 cm⁻¹) and galactose-4-sulfate moiety (844 cm⁻¹) as the proportion of dXG increases. Additionally, a comparison between kC2/dXG1 powders and their corresponding gels (Figure S2c) reveals sharper and more intense peaks in the powders. These spectral observations suggest that no strong specific interactions occur between the components, as no new peaks or significant shifts are detected. The reduced intensity of vibration bands in the gels likely reflects the restricted mobility of functional groups due to physical cross-linked network formation.

Figure 2a depicts the comparison of frequency-sweep tests on kC2-Na-K and kC2/dXG1-Na-K blends prepared through various methods. The kC2-Na-K and kC2/dXG1-Na-K (second method) exhibit similar behavior, with the formulation without dXG showing a slightly higher G' modulus. Conversely, kC2/dXG1-Na-K prepared using the first method demonstrates a higher modulus compared to kC2-Na-K, likely due to the increased polymer concentration combined with a more effective homogenization, resulting from the difference in the preparation method. As a matter of fact, the second method involves homogenization at 120°C in an oil bath for 1 h, whereas the first method allows for 5 h of homogenization before the samples were cooled

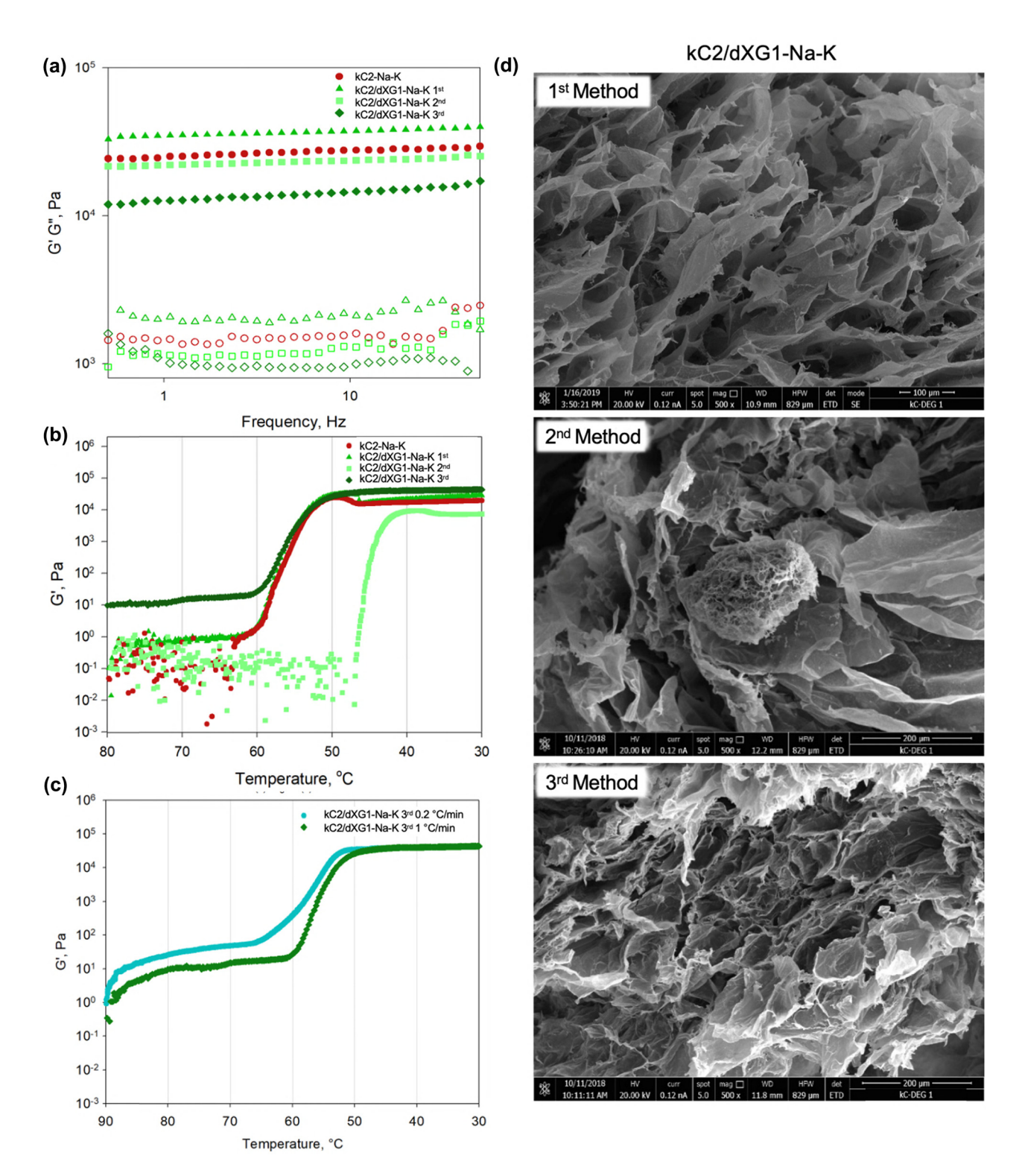


Figure 2: Storage modulus, G' (full dot), and loss modulus, G'' (hollow dot), of kC2-Na-K, and kC2/dXG1-Na-K prepared with first, second, and third methods as a function of frequency (a), as a function of temperature decreasing the temperature from 80 to 30°C at a rate of 1°C/min (b), as a function of temperature decreasing the temperature from 80 to 30°C at a rate of 0.2°C/min only for kC2/dXG1-Na-K prepared with the third method (c). (d) SEM micrographs (cross-sections) of kC2/dXG1-Na-K prepared with first, second, and third methods at 500× magnification.

down slowly to room temperature. In contrast, kC2/dXG1-Na-K prepared using the third method exhibits lower moduli, even below those obtained with the second method. This lower modulus is attributed to the insufficient time for dXG to form a network, as the solution is rapidly quenched at 15°C following homogenization at 120°C, resulting in dXG being somewhat trapped by kC and impairing the network, ultimately lowering the moduli.

Figure 2b presents a comparison of the temperature ramps for G' cooling curves for kC2-Na-K and kC2/dXG1-Na-K, all prepared using three distinct methods. Notably, the kC2/dXG1-Na-K formulation prepared by the second method, despite containing a high polymer concentration of 3% w exhibits the lowest transition temperature, similar to that observed for kC2 without any salts. This indicates that the partially dXG may not have been adequately homogenized with kC, thus hindering kC gelation. kC2/ dXG1-Na-K prepared by the first method shows a transition temperature equivalent to that of kC2-Na-K. This may suggest that the only transition being measured is that of kC. as the sample was heated to only 80°C. This observation is further corroborated by the temperature sweep curve of kC2/dXG1-Na-K produced via the third method. In this instance, the sample was initially prepared by homogenizing kC and dXG solutions, resulting in rapid gelation that did not allow dXG adequate time to establish a network within the presence of kC. However, during the temperature sweep measurement, for which the full spectrum is presented in Figure 2c, the kC2/dXG1-Na-K solution was reheated to 120°C to ensure both kC and dXG were in a sol state. The analysis of solution behavior commenced at 90°C and proceeded gradually to lower temperatures, thereby providing dXG an opportunity to form its network while kC remained in solution. This is why a transition, evidenced by an increase in G' modulus, is noted at 90°C. Upon reaching the transition point of kC2-Na-K, the moduli exhibit a further increase as a result of the kC transition. The temperature ramp test for kC2/dXG1-Na-K prepared by the third method was also conducted at a reduced cooling rate of 0.2°C/min (Figure 2c). A comparison between this scenario and the one conducted at 1°C/min reveals that the lower cooling rate grants dXG greater time to establish a structured network, leading to an enhancement in moduli. A similar phenomenon is observed in the kC component, which provides the opportunity to initiate network structuring at elevated temperatures, resulting in a less pronounced slope in the transition temperature region.

Figure 2d illustrates the morphology of kC2/dXG1-Na-K produced using the three methods. Notably, in the

formulation prepared via the second method, certain regions exhibit significantly different porosity characteristics, showcasing microporosity that is comparable to that of solely dXG [24]. The analysis indicates that the two polymers do not fully interpenetrate, resulting in distinct regions with differing characteristics. A notable variation is observed in the samples of kC2/dXG1-Na-K prepared using first and third methods. In these instances, the samples exhibit an intermediate structure between kC2-Na-K and dXG, characterized by a certain degree of microporosity. This suggests that the two polymers may form a composite structure that possesses attributes characteristic of both systems. In the first method, this behavior can likely be attributed to improved homogenization, while the third method shows rapid gelation, which inhibits the formation of individual polymer networks.

Influence of dXG concentration on kC-Na-K

As noted in the "Influence of K⁺ and Na⁺ ions on kC gelation and properties" section, the kC2-K and kC2-Na-K formulations exhibited similar characteristics, with both presenting as the strongest and most suitable options for the objectives of this study. The impact of NaN3 was found to be insignificant in the presence of KCl; therefore, kC2-Na-K was chosen for the preparation of blends with different dXG concentrations, in the context of retaining NaN3 solely as a preservative and with the hypothesis of eliminating it from the formulation when high biocompatibility is needed. Additionally, the first method was selected for all kC/dXG blends, as it likely provided a more homogeneous system and enhanced mechanical properties.

Various formulations containing different amounts of dXG, prepared using the first method, were tested to gain a deeper understanding of the influence of dXG on the overall structure. Figure 3a illustrates the quantification of transparency expressed in terms of UV-vis scattering values measured between 250 and 800 nm. The hydrogel with the highest percentage of dXG displayed the greatest absorbance and appears more turbid, while the hydrogel devoid of dXG was the clearest upon visual inspection and exhibited the lowest UV absorbance. Table 4 presents the optical density values at 500 nm for various hydrogels. Notably, the transparency of all films was maintained (Figure 3b). Transparency is a recognized property of commercial hydrogels for wound dressing, such as Neoheal® and BurnTec®, where it is considered clinically advantageous because it allows continuous inspection of the wound without removal of the dressing [45-47]. These

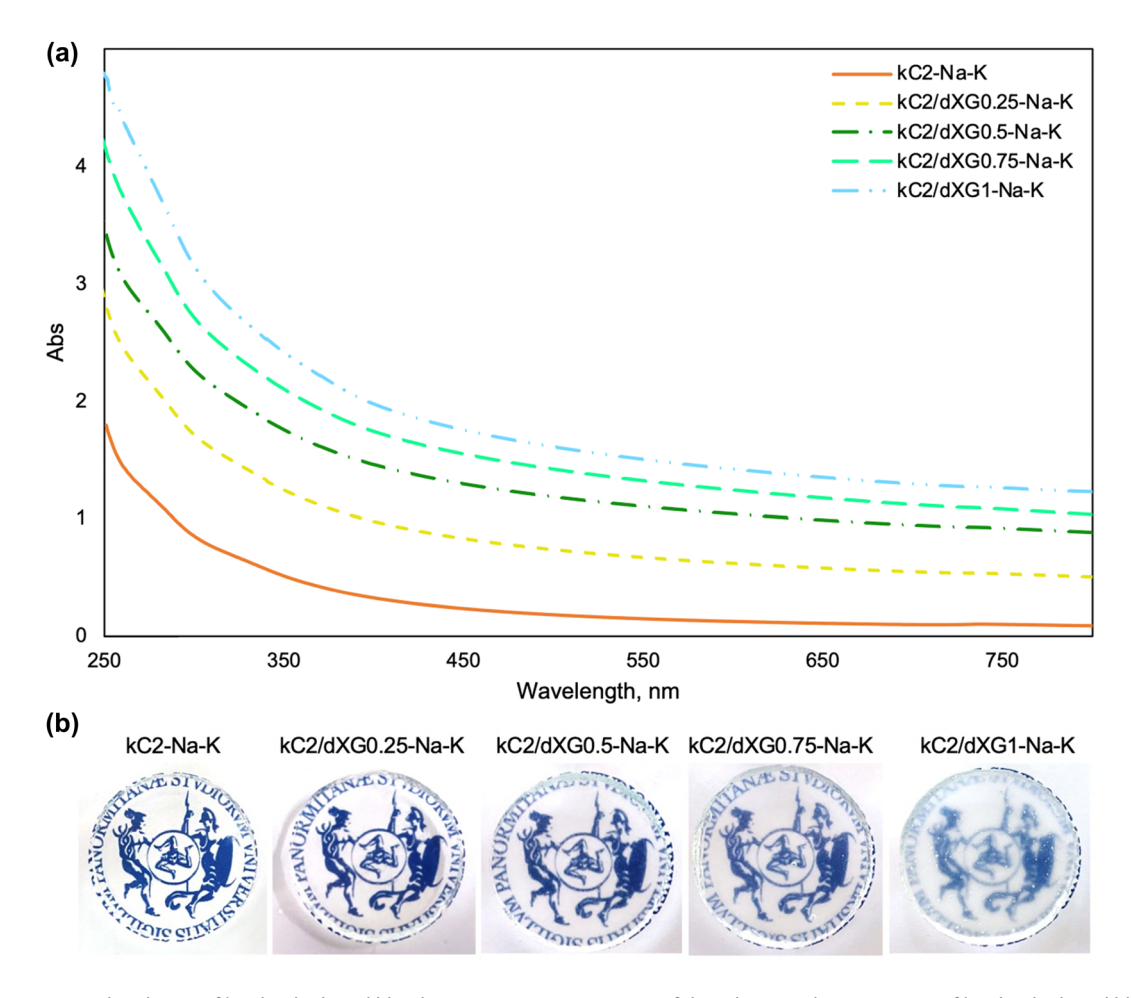


Figure 3: (a) UV-vis absorbance of kC/dXG hydrogel blends at various concentrations of dXG. (b) Optical transparency of kC/dXG hydrogel blend disks of 4 mm width.

kC/dXG blends maintained high optical clarity, particularly at a lower dXG content.

The formulations were evaluated for their swelling behavior in pure water. The results, illustrated in Figure 4a, demonstrate that all systems initially exhibit varying degrees of swelling, followed by a gradual complete erosion, likely attributed to the leaching of K⁺ ions from the network. The introduction of increasing amounts of dXG influences both the maximum swelling degree and the erosion rate. Erosion occurs most rapidly in systems with the highest dXG concentration, while the system containing 0.5% dXG shows the slowest erosion. Several concurrent factors contribute to these observations: (1) the presence of dXG may interfere with the gelation of kC, resulting in a looser network structure, especially as the quantity of dXG increases; (2) dXG forms less hydrophilic domains which can impede erosion when added in limited quantities, preventing excessive disruption of the network; (3) dXG itself exhibits limited swelling and is expected to erode slowly [20,24].

To assess the behavior of hydrogels in the presence of ions in the swelling medium, swelling and erosion tests were conducted in isotonic PBS, as illustrated in Figure 4b. Initially, all hydrogels exhibited a rapid weight increase, resulting in a lower degree of swelling compared to those in pure water, followed by a gradual weight decrease. This phenomenon may be attributed to the stabilizing effect of K^+ ions on the network, which, unlike water, allowed for increased resistance to erosion.

Table 4: Optical densities of hydrogels with various compositions measured at 500 nm wavelength

Optical density at 500 nm				
kC2-Na-K	0.18			
kC2/dXG0.25-Na-K	0.70			
kC2/dXG0.5-Na-K	1.30			
kC2/dXG0.75-Na-K	1.50			
kC2/dXG1-Na-K	1.70			

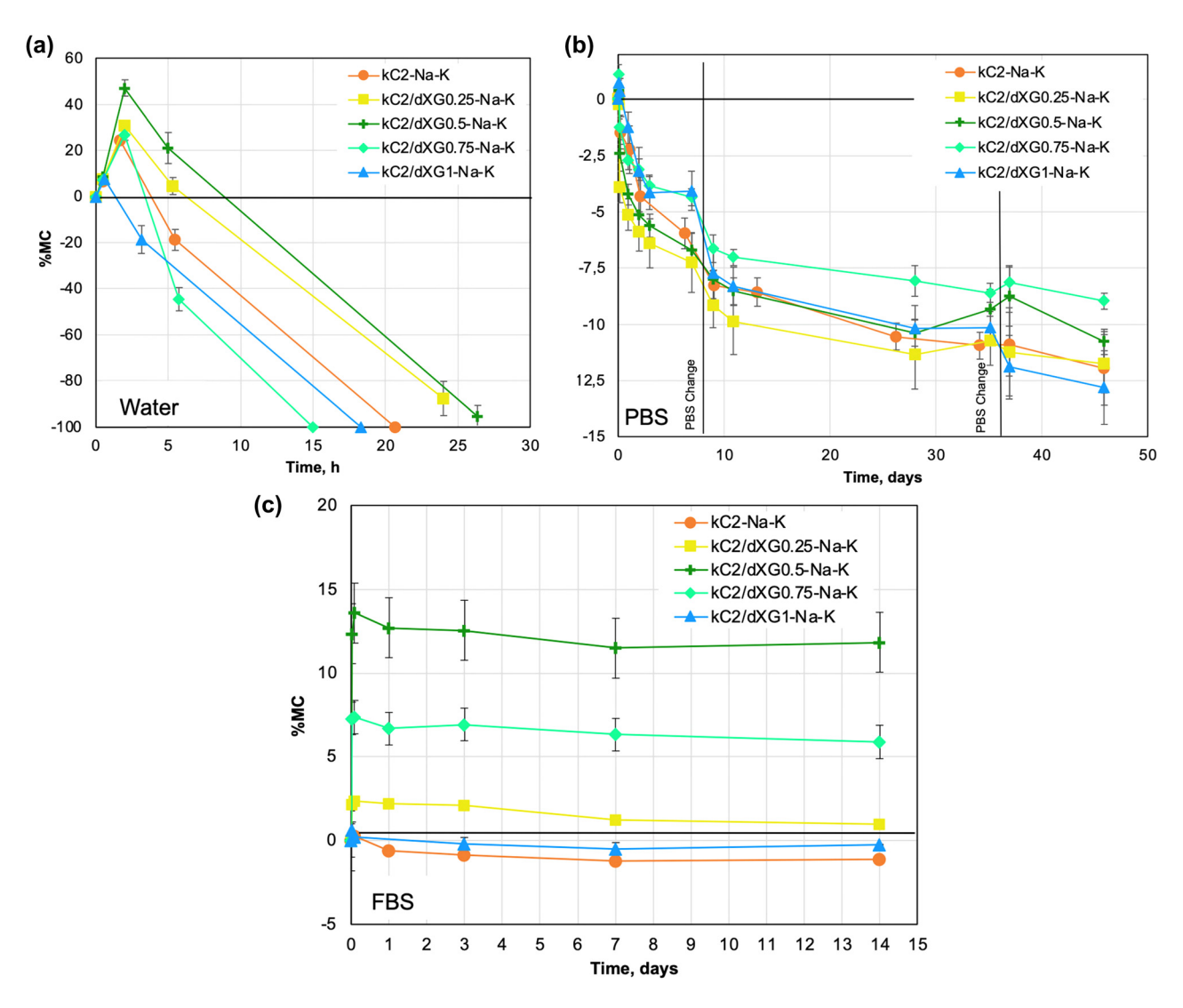


Figure 4: Swelling and erosion mass change, % MC, of kC2-Na-K, kC2/dXG0.25-Na-K, kC2/dXG0.5-Na-K, kC2/dXG0.75-Na-K, and kC2/dXG1-Na-K in 0.02% NaN₃ solution (a), PBS (b), and FBS (c) as a function of time.

Following 7 days of observation, the swelling medium was changed as the majority of the samples approached a plateau. After this medium change, the mass of the samples continued to decrease. A subsequent medium change after 5 weeks did not significantly alter the mass, likely due to the gels having leached out most of the free elements, leading to a more gradual erosion process thereafter. Hydrogels with intermediate concentrations of dXG (0.5 and 0.75%) displayed the highest degree of swelling and the lowest weight loss compared to the other formulations. Conversely, kC2/dXG0.25-Na-K and kC2/dXG1-Na-K demonstrated behavior similar to that of kC2-Na-K. kC2/dXG0. 5-Na-K and kC2/dXG0.75-Na-K maintained a more stable network than kC2/dXG0.25-Na-K, likely owing to the higher polymer concentration. However, kC2/dXG1-Na-K exhibited behavior similar to kC2-Na-K, with slightly increased

erosion due to the contrasting effects that offset one another: the disturbance of the kC network caused by dXG and the benefits of a higher polymer concentration.

To further evaluate the fluid uptake of the hydrogels in an environment that simulates conditions of human wounds, swelling and degradation testing were performed in FBS. Due to the degradation of serum components, this test was concluded after 2 weeks. In this scenario, the hydrogels containing dXG were capable of swelling beyond their original weight, achieving a maximum of 15% for kC2/dXG0.5-Na-K. Once again, the gel without dXG registered the lowest degree of swelling and experienced the greatest weight loss. Furthermore, kC2/dXG1-Na-K demonstrated behavior comparable to that of kC2-Na-K, reinforcing the notion that the highest percentage of dXG may hydrolytically destabilize the network. Although the reported

swelling values are lower than commercially available hydrogels for wound dressings, these formulations are able to maintain a moist environment while exhibiting sufficient structural integrity due to the shown hydrolytic stability, which may be rare with the natural physically crosslinked hydrogel.

To evaluate the mechanical properties of the hydrogel blend, rheological analysis was performed. Figure 5a

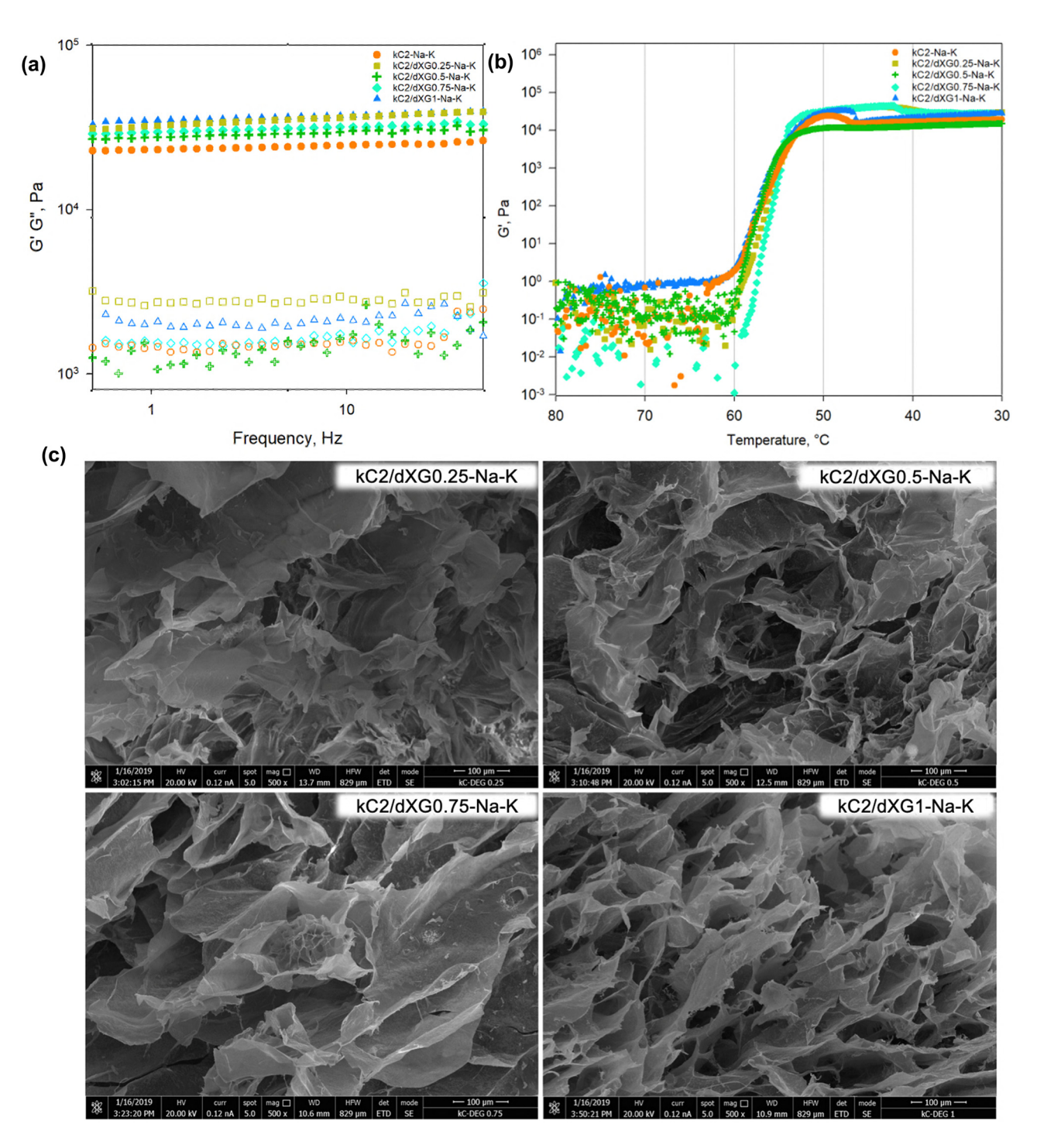


Figure 5: Storage modulus, G' (full dot), and loss modulus, G'' (hollow dot), of kC2-Na-K, kC2/dXG0.25-Na-K, kC2/dXG0.5-Na-K, kC2/dXG0.75-Na-K, and kC2/dXG1-Na-K prepared with the first method (a) as a function of frequency and (b) as a function of temperature, decreasing the temperature from 80° to 30°C at a rate of 1°C/min. (c) SEM micrographs (cross-sections) of kC2/dXG0.25-Na-K, kC2/dXG0.5-Na-K, kC2/dXG0.75-Na-K, and kC2/dXG1-Na-K prepared with the first method at 500× magnification (scale bar: 100 μ m).

presents a comparison of frequency-sweep tests conducted on kC2-Na-K, kC2/dXG0.25-Na-K, kC2/dXG0.5-Na-K, kC2/ dXG0.75-Na-K, and kC2/dXG1-Na-K, all prepared using the first method. The hydrogels containing dXG exhibited higher moduli than that with solely kC, likely due to the increased polymer concentration. All formulations showed a trend of increasing moduli with the percentage of dXG, with the exception of kC2/dXG0.25-Na-K that showed higher moduli than kC2/dXG0.5-Na-K and kC2/dXG0.75-Na-K. This could be attributed to a synergistic effect stemming from the presence of dXG, which at a concentration of 0.25% raises the polymer concentration without significantly disturbing the kC network, leading to higher moduli. In contrast, other formulations faced disturbances in the kC network that were counterbalanced by the increases in the overall polymer concentration without evidencing a synergistic effect like kC2/dXG0.25-Na-K. All formulations showed G' values within the range reported for commercial and clinically relevant hydrogels for wound dressings, which overlap with the mechanical properties of soft tissues (on the order of magnitude of 10^2 – 10^4 Pa) [46,48,49]. They are designed to have a G' sufficient to maintain integrity during handling and application, yet not excessively high, to ensure conformability to the skin surface and patient comfort.

Figure 5b compares temperature ramps for *G'* cooling curves, for kC2-Na-K, kC2/dXG0.25-Na-K, kC2/dXG0.5-Na-K, kC2/dXG0.75-Na-K, and kC2/dXG1-Na-K prepared with the first method.

All the systems examined exhibit a transition temperature consistent with kC2-Na-K, indicating that the only transition observed is the kC transition influenced by the salts. This observation is attributable to the fact that the samples prepared using this method were heated to a maximum of 80°C, a temperature insufficient for dXG to undergo a gel–sol transition, thereby remaining in a gel bead form suspended in the kC solution, as previously stated.

Figure 5c illustrates the morphology of kC2/dXG0.25-Na-K, kC2/dXG0.5-Na-K, kC2/dXG0.75-Na-K, and kC2/dXG1-Na-K, all prepared using the first method. These samples display an intermediate structure between kC2-Na-K (Figure 1d) and the dXG structure observed in previous studies [24]. The kC2/dXG0.25-Na-K sample has a structure that more closely resembles kC2-Na-K, while increasing the dXG concentration enhances the microporosity, suggesting the formation of a structure that embodies characteristics of both systems. Such morphological changes are highly relevant for wound-healing applications, as the pore size and connectivity have been linked to enhanced nutrient and oxygen diffusion, as well as improved cellular

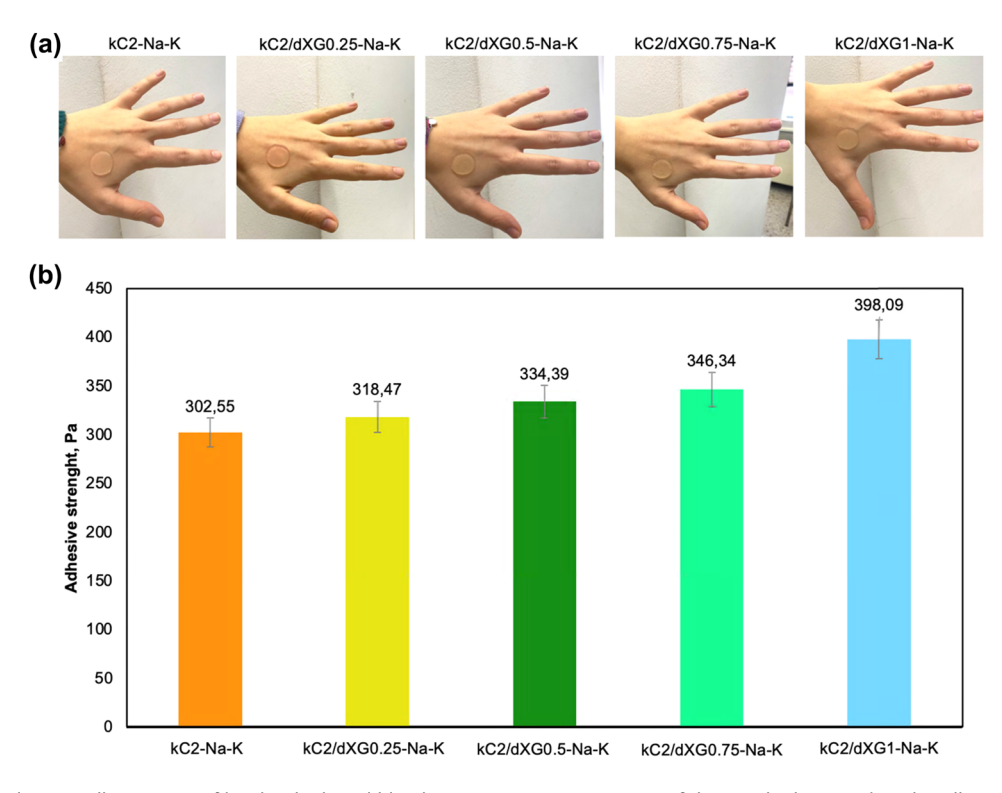


Figure 6: (a) Qualitative adhesiveness of kC/dXG hydrogel blends at various concentrations of dXG on the human skin. (b) Adhesive strength of kC/dXG hydrogel blends at various concentrations of dXG on silicon synthetic skin.

infiltration and tissue integration [49]. Thus, the observed increase in microporosity with rising dXG content not only reflects the interplay between the two polysaccharides but may also contribute to the functional performance of these hydrogels as wound dressings.

To verify if dXG confers more adhesiveness to kC, the adhesive strength of the hydrogels was assessed using synthetic silicon skin as the adhesion substrate. As shown in Figure 6, the adhesive strength of the formulations ranged from 300 to 400 Pa, with kC2/dXG1 demonstrating the highest adhesiveness. Notably, adhesiveness tends to increase with higher concentrations of dXG, likely due to the intrinsic adhesive properties of the polysaccharide [25,26]. This range of adhesive levels is not very strong and may facilitate the gentle and atraumatic removal of the gel from the wound bed post-application, maybe in combination with gauze. This approach is also explicitly recommended in wound-care guidelines and by manufacturers of commercial hydrogels such as Neoheal® and BurnTec® (KikGel, Poland), which are applied in contact with the wound bed and then covered with a secondary dressing to ensure stability [46,47].

Conclusions

This research explores the synergistic effects of dXG and kC for possible wound healing applications. To this aim, the formulations must fulfill several requirements related to both their processing conditions and their application. Swelling, erosion, rheology, FTIR, UV-vis, SEM, and adhesion tests were performed on the hydrogels, to understand how they can be adjusted to become suitable for the envisaged application. The FTIR analysis evidenced the absence of specific physico-chemical interactions between the two polymeric components in the formulations. The presence of K⁺ ions in the formulation favored the formation of a more stable and ordered gel network, and the preparation method played a key role in determining the properties of the final gels. In the case of prolonged homogenization, the first method - which entailed prolonged stirring of the blend and slow cooling - provided the most homogeneous and mechanically strong hydrogels and was selected for the preparation of the blends. The hydrogels containing dXG demonstrated increased swelling capacity in FBS, a medium which imitates real biological environments and wound exudates. Furthermore, they presented increased adhesiveness with increasing dXG concentration. Also, the morphology benefited from the addition of dXG that granted a more porous structure to the kC.

Among all formulations, when the concentration of dXG was within the range of 0.5–0.75%, such hydrogel blends combined acceptable mechanical properties and adhesiveness with hydrolytic stability and the advantage of transparency, which are important attributes if they were to be used as wound dressings.

It is evident that the combination of kC with dXG, especially under controlled homogenization preparation, offers an excellent route to develop natural, entirely biobased, and biocompatible hydrogels with good mechanical strength, adhesiveness, and transparency. Such properties make kC/dXG hydrogels a perfect candidate for wound healing applications.

Optimization of polymer concentrations and further evaluation in long-term biocompatibility *in vitro* and *in vivo* will be the point of future research.

Funding information: Emanuela Muscolino was funded by the European Union – NextGenerationEU through the Italian Ministry of University and Research under the PNRR – M4C2-I1.3 Project PE_00000019 "HEAL ITALIA" CUP B73C22001250006. The ideas voiced are just those of the authors and do not automatically reveal those of the European Commission or the European Union. Neither the European Commission nor the European Union should be held accountable for them.

Author contributions: Conceptualization, data curation, investigation, methodology, project administration, validation, visualization, and writing – original draft were done by Emanuela Muscolino. Funding acquisition, resources, supervision, writing – review and editing were done by Clelia Dispenza. All authors read and approved the final manuscript.

Conflict of interest: The authors state no conflict of interest.

Data availability statement: The datasets generated during and/or analyzed during the current study are available from the corresponding author on reasonable request.

References

- [1] Özbaş Z, Özkahraman B, Bayrak G, Kılıç Süloğlu A, Perçin I, Boran F, et al. Poly(vinyl alcohol)/(hyaluronic acid-g-kappa-carrageenan) hydrogel as antibiotic-releasing wound dressing. Chem Pap. 2021;75:6591–600.
- [2] Singh P, Verma C, Mukhopadhyay S, Gupta A, Gupta B. Preparation of thyme oil loaded κ-carrageenan-polyethylene glycol hydrogel membranes as wound care system. Int J Pharm. 2022;618:121661.

- [3] Neamtu B, Barbu A, Negrea MO, Berghea-Neamtu CS, Popescu D, Zăhan M, et al. Carrageenan-based compounds as wound healing materials. Int J Mol Sci. 2022;23:9117.
- [4] Wang H, Zhang L-M. Intelligent biobased hydrogels for diabetic wound healing: A review. Chem Eng J. 2024;484:149493.
- Wang P, Cai F, Li Y, Yang X, Feng R, Lu H, et al. Emerging trends in the application of hydrogel-based biomaterials for enhanced wound healing: A literature review. Int J Biol Macromol. 2024;261:129300.
- Verma D, Okhawilai M, Nangan S, Thakur VK, Gopi S, Kuppusamy K, et al. A sustainable and green approach towards the utilization of biopolymers for effective wound dressing applications: A detailed review. Nano-Struct Nano-Objects. 2024;37:101086.
- Şen M, Avcı EN. Radiation synthesis of poly(N -vinyl-2pyrrolidone)-ĸ-carrageenan hydrogels and their use in wound dressing applications. I. Preliminary laboratory tests. J Biomed Mater Res A. 2005;74A:187-96.
- Fahmy HM, Aly AA, Sayed SM, Abou-Okeil A. K-carrageenan/Naalginate wound dressing with sustainable drug delivery properties. Polym Adv Technol. 2021;32:1793-801.
- Li X-X, Dong J-Y, Li Y-H, Zhong J, Yu H, Yu Q-Q, et al. Fabrication of Ag-ZnO@ carboxymethyl cellulose/K-carrageenan/graphene oxide/konjac glucomannan hydrogel for effective wound dressing in nursing care for diabetic foot ulcers. Appl Nanosci. 2020;10:729-38.
- [10] Zhang Y, Ye L, Cui M, Yang B, Li J, Sun H, et al. Physically crosslinked poly(vinyl alcohol)-carrageenan composite hydrogels: pore structure stability and cell adhesive ability. RSC Adv. 2015;5:78180-91.
- [11] Kara S, Tamerler C, Bermek H, Pekcan Ö. Cation effects on sol-gel and gel-sol phase transitions of κ-carrageenan-water system. Int J Biol Macromol. 2003;31:177-85.
- [12] Mangione MR, Giacomazza D, Bulone D, Martorana V, Cavallaro G, San Biagio PL. K⁺ and Na⁺ effects on the gelation properties of κ-Carrageenan. Biophys Chem. 2005;113:129-35.
- [13] Ulagesan S, Krishnan S, Nam T-J, Choi Y-H. The influence of κ-Carrageenan-R-phycoerythrin hydrogel on in vitro wound healing and biological function. Int J Mol Sci. 2023;24:12358.
- [14] Shirakawa M, Yamatoya K, Nishinari K. Tailoring of xyloglucan properties using an enzyme. Food Hydrocoll. 1998;12:25-8.
- [15] Todaro S, Dispenza C, Sabatino MA, Ortore MG, Passantino R, San Biagio PL, et al. Temperature-induced self-assembly of degalactosylated xyloglucan at low concentration. J Polym Sci Part B Polym Phys. 2015;53:1727-35.
- [16] Han M, Liu Y, Zhang F, Sun D, Jiang J. Effect of galactose side-chain on the self-assembly of xyloglucan macromolecule. Carbohydr Polym. 2020;246:116577.
- [17] Todaro S, Sabatino MA, Mangione MR, Picone P, Di Giacinto ML, Bulone D, et al. Temporal control of xyloglucan self-assembly into layered structures by radiation-induced degradation. Carbohydr Polym. 2016;152:382-90.
- Muscolino E, Sabatino MA, Jonsson M, Dispenza C. The role of water in radiation-induced fragmentation of cellulosic backbone polysaccharides. Cellulose. 2023;31(2):841-56. doi: 10.1007/s10570-023-05660-4
- [19] Dispenza C, Todaro S, Bulone D, Sabatino MA, Ghersi G, San Biagio PL, et al. Physico-chemical and mechanical characterization of in-situ forming xyloglucan gels incorporating a growth factor to promote cartilage reconstruction. Mater Sci Eng C. 2017;70:745-52.
- [20] Toia F, Di Stefano AB, Muscolino E, Sabatino MA, Giacomazza D, Moschella F, et al. In-situ gelling xyloglucan formulations as 3D

- artificial niche for adipose stem cell spheroids. Int | Biol Macromol. 2020:165:2886-99.
- [21] Muscolino E, Di Stefano AB, Toia F, Giacomazza D, Moschella F, Cordova A, et al. Xyloglucan, alginate and k-carrageenan hydrogels on spheroids of adipose stem cells survival; preparation, mechanical characterization, morphological analysis and injectability. Carbohydr Polym Technol Appl. 2024;8:100566.
- Picone P, Muscolino E, Girgenti A, Testa M, Giacomazza D, Dispenza C, et al. Mitochondria embedded in degalactosylated xyloglucan hydrogels to improve mitochondrial transplantation. Carbohydr Polym Technol Appl. 2024;8:100543.
- [23] Di Stefano AB, Muscolino E, Trapani M, Moschella F, Corradino B, Toia F, et al. Partially degalactosylated xyloglucan hydrogel artificial niches enhance human spheroids derived from adipose stem cells stemness and differentiation potential. Carbohydr Polym Technol Appl. 2025;9:100652.
- [24] Muscolino E, Di Stefano AB, Trapani M, Sabatino MA, Giacomazza D, Moschella F, et al. Injectable xyloglucan hydrogels incorporating spheroids of adipose stem cells for bone and cartilage regeneration. Mater Sci Eng C. 2021;131:112545.
- Fry SC. The growing plant cell wall: chemical and metabolic [25] analysis. 1. publ. Harlow: Longman Scientific & Technical; 1988.
- Zhou Q, Rutland MW, Teeri TT, Brumer H. Xyloglucan in cellulose [26] modification. Cellulose. 2007;14:625-41.
- Zhao Z, Crespi VH, Kubicki JD, Cosgrove DJ, Zhong L. Molecular dynamics simulation study of xyloglucan adsorption on cellulose surfaces: effects of surface hydrophobicity and side-chain variation. Cellulose. 2014;21:1025-39.
- [28] do Rosário MMT, Noleto GR, de Oliveira Petkowicz CL. Degalactosylation of xyloglucans modify their pro-inflammatory properties on murine peritoneal macrophages. Int J Biol Macromol.
- [29] Esquena-Moret J. A review of xyloglucan: Self-aggregation, hydrogel formation, mucoadhesion and uses in medical devices. Macromol. 2022;2:562-90.
- [30] Miyazaki S, Kawasaki N, Kubo W, Endo K, Attwood D. Comparison of in situ gelling formulations for the oral delivery of cimetidine. Int J Pharm. 2001;220:161-8.
- [31] Miyazaki S, Suzuki S, Kawasaki N, Endo K, Takahashi A, Attwood D. In situ gelling xyloglucan formulations for sustained release ocular delivery of pilocarpine hydrochloride. Int J Pharm. 2001;229:29-36.
- [32] Miyazaki S, Suisha F, Kawasaki N, Shirakawa M, Yamatoya K, Attwood D. Thermally reversible xyloglucan gels as vehicles for rectal drug delivery. J Controlled Rel. 1998;56:75-83.
- [33] Gulino F, Muscolino E, Alessi S, Nuzzo D, Picone P, Giacomazza D, et al. Hydrogel dressings with egg white proteins for wound healing. Chem Eng Trans. 2024;110:247-52.
- Picone P, Sanfilippo T, Vasto S, Baldassano S, Guggino R, Nuzzo D, [34] et al. From small peptides to large proteins against Alzheimer's disease. Biomolecules. 2022;12:1344.
- Muscolino E, Di Stefano AB, Trapani M, Sabatino MA, Giacomazza D, [35] Alessi S, et al. κ-Carrageenan and PVA blends as bioinks to 3D print scaffolds for cartilage reconstruction. Int J Biol Macromol. 2022;222:1861-75.
- [36] Muscolino E, Costa MA, Sabatino MA, Alessi S, Bulone D, San Biagio PL, et al. Recombinant mussel protein Pvfp5β enhances cell adhesion of poly(vinyl alcohol)/k-carrageenan hydrogel scaffolds. Int | Biol Macromol. 2022;211:639-52.
- [37] Picone P, Sabatino MA, Ajovalasit A, Giacomazza D, Dispenza C, Di Carlo M. Biocompatibility, hemocompatibility and antimicrobial

- properties of xyloglucan-based hydrogel film for wound healing application. Int J Biol Macromol. 2019;121:784–95.
- [38] Yegappan R, Selvaprithiviraj V, Amirthalingam S, Jayakumar R. Carrageenan based hydrogels for drug delivery, tissue engineering and wound healing. Carbohydr Polym. 2018;198:385–400.
- [39] Galvano S, Di Stefano AB, Muscolino E, Trapani M, Toia F, Dispenza C. Development of adaptable 3D-bioprinted scaffold for tissue regeneration. Chem Eng Trans. 2024;110:253–8.
- [40] Brun-Graeppi AK, Richard C, Bessodes M, Scherman D, Narita T, Ducouret G, et al. Study on the sol–gel transition of xyloglucan hydrogels. Carbohydr Polym. 2010;80:555–62.
- [41] Volery P, Besson R, Schaffer-Lequart C. Characterization of commercial carrageenans by fourier transform infrared spectroscopy using single-reflection attenuated total reflection. J Agric Food Chem. 2004;52:7457–63.
- [42] Kara S, Tamerler C, Pekcan Ö. Cation effects on swelling of κ-carrageenan: A photon transmission study. Biopolymers. 2003;70:240–51.

- [43] Kara S, Tamerler C, Bermek H, Pekcan Ö. Hysteresis during sol-gel and gel-sol phase transitions of k-Carrageenan: A photon transmission study. J Bioact Compat Polym. 2003;18:33–44.
- [44] Liu J, Willför S, Xu C. A review of bioactive plant polysaccharides: Biological activities, functionalization, and biomedical applications. Bioact Carbohydr Diet Fibre. 2015;5:31–61.
- [45] Kuddushi M, Shah AA, Ayranci C, Zhang X. Recent advances in novel materials and techniques for developing transparent wound dressings. | Mater Chem B. 2023;11:6201–24.
- [46] Neoheal[®]. Hydrogel dressing for wound management. KIKGEL. https://kikgel.com.pl/en/products/neoheal/. Accessed 25 Aug 2025.
- [47] BurnTec[®]. First aid dressings for burns and skin injuries. KIKGEL. https://kikqel.com.pl/en/products/burntec/. Accessed 25 Aug 2025.
- [48] Norahan MH, Pedroza-González SC, Sánchez-Salazar MG, Álvarez MM, Trujillo De Santiago G. Structural and biological engineering of 3D hydrogels for wound healing. Bioact Mater. 2023;24:197–235.
- [49] Demeter M, Scărișoreanu A, Călina I. State of the art of hydrogel wound dressings developed by ionizing radiation. Gels. 2023;9:55.